Available online at www.sciencedirect.com
ScienceDirect
Cement and Concrete Research 36 (2006) 1603–1608
Cement and Concrete Research

Bleeding of concrete as an ageing consolidation process

Laurent Josserand [a,*], Olivier Coussy [b], François de Larrard [c]

[a] Polytech'orleans, 8 rue Leonard de Vinci, 45072, Orleans Cedex 2, France
[b] Institut Navier, Laboratoire Central des Ponts et Chaussées (LCPC), France
[c] Laboratoire Central des Ponts et Chaussées (LCPC), France

Received 13 November 2003; accepted 4 October 2004

Abstract

Bleeding of concrete results mainly from the self-weight consolidation of the granular skeleton. Simultaneous physical and chemical structural effects provoke the ageing of the skeleton. In addition, the displacements are large and the hydromechanical properties evolve locally with the porosity. All these phenomena are here addressed through an ageing nonlinear model accounting for the sample size effect experimentally observed on the bleeding capacity. The characteristic time scaling of the ageing effect is found to be dependent mainly upon the amount of cement in the mix-design and the temperature. It appears to be a key indicator for assessing the properties of fresh concretes and their evolution in time.

Keywords: Bleeding; Fresh concrete; Ageing; Calculations; Permeability

1. Introduction

Bleeding is the accumulation of water at the surface of cement-based materials. In some case, a thin layer of clear water appears only half an hour after casting a concrete piece. Bleeding has a major impact on the long-term durability of concrete since excessive bleeding weakens the bond between cement matrix and the subsurface of aggregates and induces a nonuniformity of strength associated with the nonuniformity of solid volume proportion.

Gravitation is the driving force at the origin of bleeding. It induces the settlement of the solid particles, provoking in turn the upward displacement of water [1]. This upward displacement occurs either uniformly or through vertical channels [2,3]. In the former case, as it is experimentally observed in Fig. 1, the height of water increases with time initially at a constant rate, irrespective of the initial height, and the rate slowly decreases to zero. The usual initial solid volume proportion ranges from 0.75 to 0.9 so that the solid particles are subjected to strong interaction forces and form a solid skeleton from the onset of the bleeding process. Accordingly, bleeding must be thought more as a consolidation process rather than a sedimentation one. The final amount of bleeding is the thickness of the layer of water which results from the overall process as time goes to infinity. It is called the bleeding capacity and is noted as ΔH_∞ since it also changes with the initial height H_0 of the solid particles consecutive to the consolidation process.

Many authors have proposed a quantitative approach to bleeding using the self-weight consolidation theory widely developed in soils mechanics [6–8]. In particular, Tan et al. [7] have proposed a model for the bleeding phenomenon with the assumption of infinitesimal transformations. They later introduced an empirical parameter to capture the ageing effect associated with the hydration of cement [4]. As observed in Fig. 2 for the mix-design detailed in Table 1, many experiments have shown that the bleeding capacity ΔH_∞ plotted against the initial height H_0 is always convex, even for slurries, mortars and concrete [3,5]. The order of magnitude of the bleeding solid volume proportion, when compared to the initial height, makes the hypothesis of infinitesimal transformations questionable. Accordingly, this paper first improves the self-weight consolidation approach

* Corresponding author. Tel.: +33 238494392; fax: +33 238417063.
E-mail address: laurent.josserand@univ-orleans.fr (L. Josserand).

0008-8846/$ - see front matter © 2004 Elsevier Ltd. All rights reserved.
doi:10.1016/j.cemconres.2004.10.006

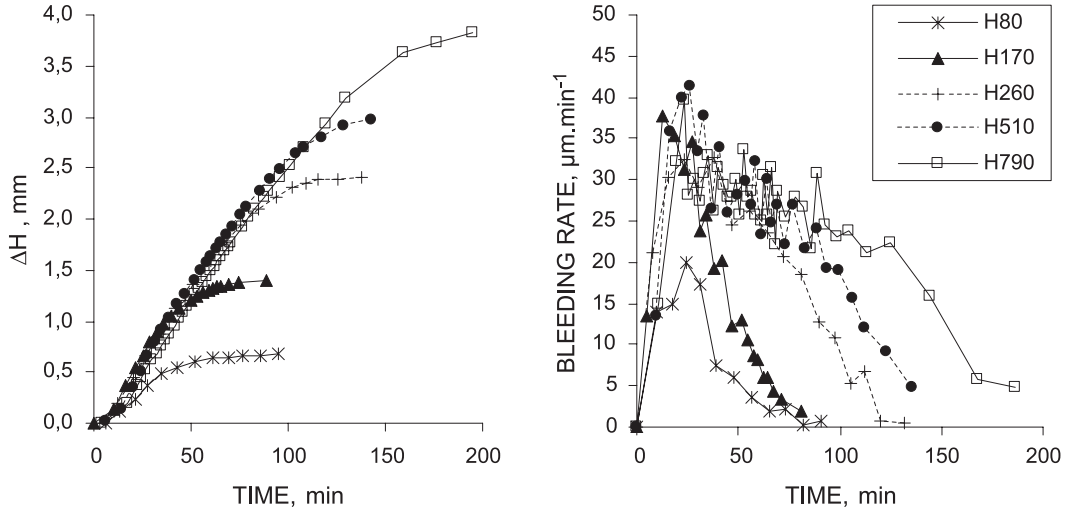

Fig. 1. Experimental curves of bleeding (left) and bleeding rates (right) for the concrete B1 (its mix-design is given in Table 1) and various initial heights (H170 stands for a 170-mm initial height).

of Tan et al. by considering finite transformations. This approach allows us to introduce an ageing effect that will be apt to account for the convexity of the bleeding capacity curve. The origins of the ageing effect and its governing parameters can be then conveniently investigated through the analysis of the variations of the characteristic time capturing the ageing kinetics.

2. An ageing self-weighted consolidation approach to bleeding

2.1. A consolidation model in finite transformations

We address here the bleeding 1D-problem of a vertical column of fresh concrete formed by the particles constituting the solid skeleton (index s) and by the liquid water saturating the remaining space (index w). Let $V_s(z, t)$ be the velocity of the solid particles at height z and time t, and $\varphi(z, t)$ the corresponding solid volume proportion such that the volume of solid forming the layer of thickness dz is φdz. Assuming the incompressibility of the solid particles, the skeleton mass balance reduces to a volume balance:

$$\frac{\partial \varphi}{\partial t} + \frac{\partial (\varphi V_s)}{\partial z} = 0. \tag{1}$$

Assuming in addition the incompressibility of the liquid water flow, the upward flow of water must be the opposite of the downward flow of solid particles.

$$(1-\varphi)V_w + \varphi V_s = 0. \tag{2}$$

The water flow is assumed to be governed by Darcy's law according to:

$$(1-\varphi)(V_w - V_s) = -K(\varphi)\left(\frac{\partial}{\partial z}\left(\frac{p}{\gamma_w}\right) + 1\right) \tag{3}$$

where $K(\varphi)$ is the current hydraulic conductivity, p is the liquid pressure and γ_w is the water specific weight. Eqs. (2) and (3) combine to:

$$V_s = K(\varphi)\left(\frac{\partial}{\partial z}\left(\frac{p}{\gamma_w}\right) - 1\right). \tag{4}$$

The vertical equilibrium requires:

$$\frac{\partial \sigma}{\partial z} + \varphi\gamma_s + (1-\varphi)\gamma_w = 0 \tag{5}$$

where σ is the vertical overall stress, compression being counted positively. Eqs. (4) and (5) combine to:

$$V_s = -\varphi K(\varphi)\left(\frac{\gamma_s}{\gamma_w} - 1\right) - \frac{K(\varphi)}{\gamma_w}\frac{\partial \sigma'}{\partial z} \tag{6}$$

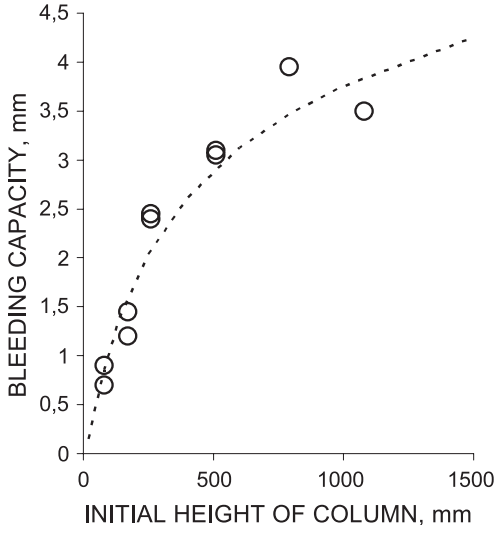

Fig. 2. Observed (circles) and predicted (dotted line) bleeding capacity of B1 as a function of the column initial height (see concrete mix-design in Table 1).

Table 1
Concrete mix-design (mass per unit volume)

Concrete	Cement	Sand 0/4	Gravel 3/8	Gravel 8/20	Water	SP[a]
B1	345	713	305	679	237	0
B2	204	778	333	742	220	0
B3	491	657	282	626	236	0
B4	453	720	312	574	229	4.55

[a] Mass of the polyacrylate high-range water reducer.

where σ' denotes Terzaghi's effective stress, usual concept in soil mechanics:

$$\sigma' = \sigma - p. \tag{7}$$

The bleeding rate V_{IR} is the opposite of the solid particle velocity V_s:

$$V_{IR} = \varphi K(\varphi)\left(\frac{\gamma_s}{\gamma_y} - 1\right) + \frac{K(\varphi)}{\gamma_w}\frac{\partial \sigma'}{\partial z}. \tag{8}$$

According to Eq. (8), the bleeding rate can be split into two terms. The first term, $\varphi K(\gamma_s/\gamma_w - 1)$, is irrespective of depth and accounts for the bleeding rate resulting from gravity and from the uplift Archimedes force. The second term, $\frac{K}{\gamma_W}\frac{\partial \sigma'}{\partial z}$, accounts for the bleeding rate resulting from the compaction of the solid skeleton. At initial time t=0, assuming uniform initial conditions within the column, the initial effective stress σ' is constant with depth so that we recover the initial bleeding rate derived by Powers [1]:

$$V_{IR}(t=0) = \Phi_0 K(\Phi_0)\left(\frac{\gamma_s}{\gamma_w} - 1\right) \tag{9}$$

where Φ_0 stands for the initial solid volume proportion. Note that $V_{IR}(t=0)$ is independent of the initial height as observed in Fig. 1. If the entrapped air is not neglected, Eq. (9) has to be corrected by removing from the right hand member the amount of air entrapped. However, this effect turns out to be generally negligible [3]. In addition, the initial rate of bleeding can be predicted according to Eq. (9) and compared with the predictions provided from the analysis of the mix-design parameters [9].

The solid particles forming at time t the layer located at height z formed, at initial time t=0, the layer located at height Z. Therefore, we can refer the solid volume proportion to the initial height and introduce the solid volume proportion function $\Phi(Z, t)$ according to:

$$\Phi(Z,t) = \varphi(z(Z),t). \tag{10}$$

The volume conservation of the solid particles forming the layer located at height z can be then expressed in the form:

$$\Phi dz = \Phi_0 dZ. \tag{11}$$

Since $dz/dt = V_s$, a time derivation of Eq. (10) and Eq. (1) combine to:

$$\frac{\partial \Phi}{\partial t} = -\frac{\Phi^2}{\Phi_0}\frac{\partial V_s}{\partial Z}. \tag{12}$$

Substitution of Eq. (12) into Eq. (6) and use of Eq. (11) finally provide:

$$\frac{\partial(\Phi_0/\Phi)}{\partial t} = -\frac{\partial}{\partial Z}\left[K(\Phi)\frac{\Phi}{\Phi_0}\left(\frac{1}{\gamma_w}\frac{\partial \sigma'}{\partial Z} + \Phi_0\left(\frac{\gamma_s}{\gamma_w} - 1\right)\right)\right] \tag{13}$$

to which we add the boundary and initial conditions:

$$\Phi(Z = H_0, t = 0) = \Phi(Z, t = 0) = \Phi_0. \tag{14}$$

From Eq. (10), the current bleeding $\Delta H(t) = H_0 - H(t)$ can be expressed in the simple form:

$$\Delta H(t) = H_0 - \int_0^{H_0} \frac{\Phi_0}{\Phi(Z,t)} dZ \tag{15}$$

2.2. An ageing model for bleeding

Once known, the solution in $\Phi(t)$ of Eq. (13), the bleeding capacity $\Delta H_\infty = \Delta H(t \to \infty)$ can be derived by letting the time go to infinity in Eq. (15). This requires the specification of the constitutive equation. We write:

$$d\sigma' = \frac{d\Phi}{C_s(\Phi)G(t)}. \tag{16}$$

Function $C_s(\Phi)$ accounts for the tangent oedometric compressibility in the absence of any ageing, while $G(t)$ is an ageing function and accounts for the stiffening of the skeleton resulting from the hydration process at the very

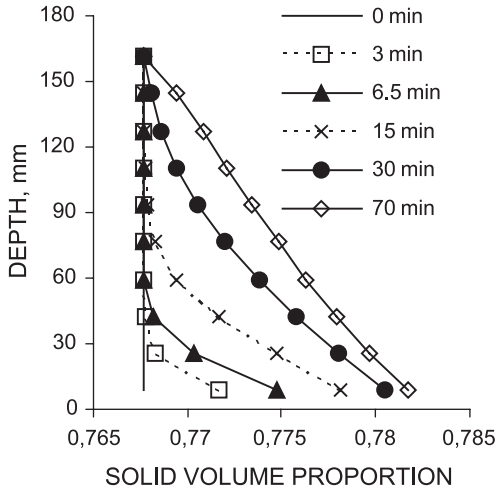

Fig. 3. Solid volume proportion profiles at various times for a 170-mm-high mould.

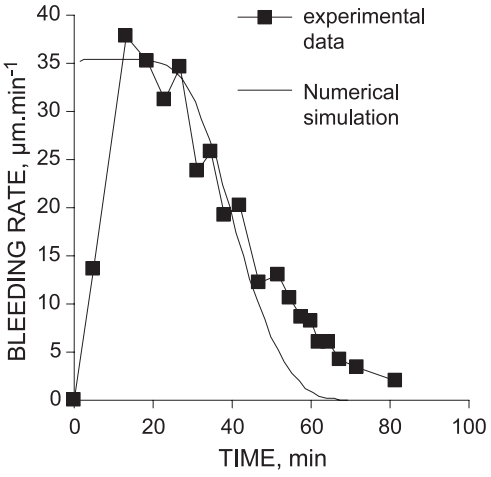

Fig. 4. Comparison of experimental and predicted bleeding rate for the 170-mm-high mould.

early ages. If we assume that the stiffening rate decreases with time, we can adopt for $G(t)$ the expression:

$$G(t) = \exp\left(-\frac{t}{T_X}\right) \tag{17}$$

where T_X is a characteristic time scaling the ageing effect. The greater T_X, the slower the ageing phenomenon is.

3. Experimental validation

Eqs. (13)–(16) form a closed set of equations. Characteristic time T_X can be taken as constant in order to capture the timescale of the ageing process from the experiments. Permeability $K(\Phi)$ and coefficient of compressibility $C_s(\Phi)$ can be assessed as functions of the solid volume proportion Φ from submodels involving the concrete mix-design parameters [3,9].

The first concrete mix-design, noted B1, we studied is given in Table 1. We chose a pure Portland cement with no mineral admixtures. All aggregate particles were rounded. An original bleeding measurement method was used [5,10]. It essentially consists in sucking water in tracks made on the top surface of the concrete.

The amount of entrapped air was found to be equal to 1.2%. The initial solid volume proportion of this mix-design is 0.768. The average specific gravity of particles is 2.66. Corresponding histories of bleeding and of associated bleeding rate are represented in Fig. 1. The observed initial bleeding rate is 37 µm min^{-1} so that, according to Eq. (9), the value of the initial permeability $K(\Phi_0)$ is 48×10^{-8} m s^{-1}. Owing to the low accuracy of permeability measurement, this value compares well with the value 33×10^{-8} m s^{-1} furnished by the model presented in Ref. [9]. Using this model to assess the permeability function $K(\Phi_0)$ for the whole range of solid volume proportion and for this particular mix-design, we write:

$$K(\Phi) = K(\Phi_0)[1 - 34(\Phi - \Phi_0)]. \tag{18}$$

Another model presented in Ref. [3] and based on the Compressible Packing Model [11] provides the compressibility function of the granular skeleton $C_s(\Phi)$ in the form:

$$C_s(\Phi) = \lambda \times 10^{-5}\exp\left(\frac{C - \Phi}{\lambda}\right). \tag{19}$$

In this last equation, C is the maximum solid volume proportion of the granular skeleton. In practice, the value of the parameter λ is found to be weakly dependent on the mix-design. Accordingly, for all the mix-designs considered in the following, we adopted the value 0.0072, obtained for the particular first mix-design of Table 1 using the Compressible Packing Model [11].

Two properties, namely, the characteristic ageing time T_X and the maximum solid volume proportion C, remain to be determined from the experimental data. Their assessment is obtained by looking for the values providing the best prediction (Eq. (15)) of the observed bleeding capacity as a function of the initial sample height H_0, that is $\Delta H_\infty = \Delta H_{t\to\infty}(H_0)$. The experimental data related to B1, the first mix-design of Table 1 are well accounted for by adopting T_X=17 min and C=0.822, producing the dotted curve in Fig. 2. These results give confidence in the general

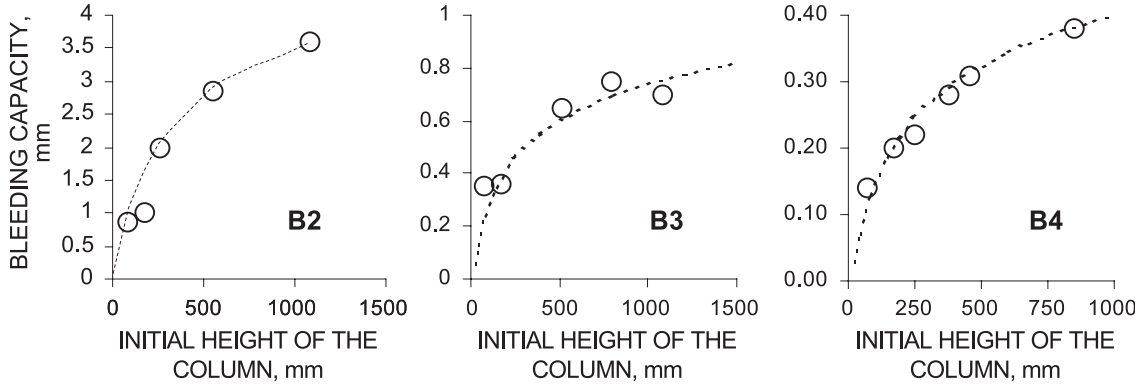

Fig. 5. Observed (circles) and predicted (dashed lines) bleeding capacity as a function of the initial height (corresponding concrete mix-designs are given in Table 1).

Table 2
Main measured and assessed data

Concrete	Φ_0	Ψ_0[a] (%)	V_{IR} (μm min^{-1})	C	T_X (min)
B1	0.768	1.2	37.0	0.822	17
B2	0.783	1.5	20.5	0.838	22
B3	0.763	1.6	8.5	0.812	12
B4	0.767	1.8	1.6	0.81	33

[a] Ψ_0 is the initial fraction of entrapped air.

approach since the value 0.822 so obtained for the maximum solid volume proportion C is not too different from the value 0.795 that can be predicted from the Compressible Packing Model [11].

Adopting the above set of values for the numerical solution of Eqs. (13)–(17), the solid volume proportion profile Φ can be derived as a function as time for various depths. The resulting curves are given in Fig. 3 for B1.

The bleeding rate as a function of time can be predicted from the predicted solid volume proportion profiles $\Phi(Z, t)$ and compares well with the observed bleeding rate history, as shown in Fig. 4, where the rising starting part of the experimental curve is due to a delay caused by the filling up by surface micropuddles [10].

The same analysis has been carried out for various mix-designs. For the three other mix-designs, B2, B3, B4, whose properties are reported in Table 1, we present, in Fig. 5, the observed and predicted bleeding capacity as a function of the initial height and, in Table 2, the main observed and assessed data related to the bleeding process.

4. Parameters influencing the characteristic time

The dependence of the characteristic ageing time T_X upon the mix-design reported in Table 2 occurs likely through two main processes, the cement hydration and the physical interactions slowly inducing a flocculent state. Both processes are particularly sensitive to the total mass of cement, as captured in Fig. 6, where T_X is plotted against the cement amount per volume unit.

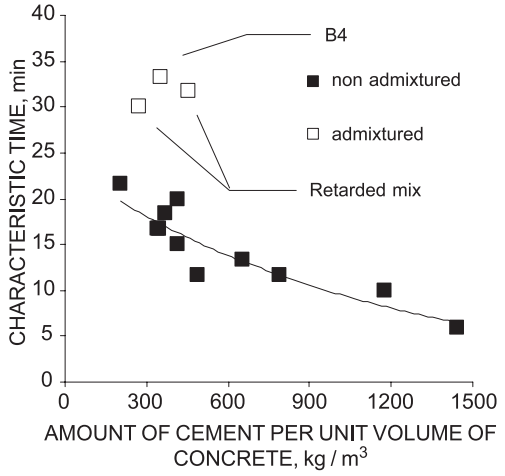

Fig. 6. Influence of the amount of cement per unit volume of concrete on the value of the characteristic time. Comparison with admixtured mixes.

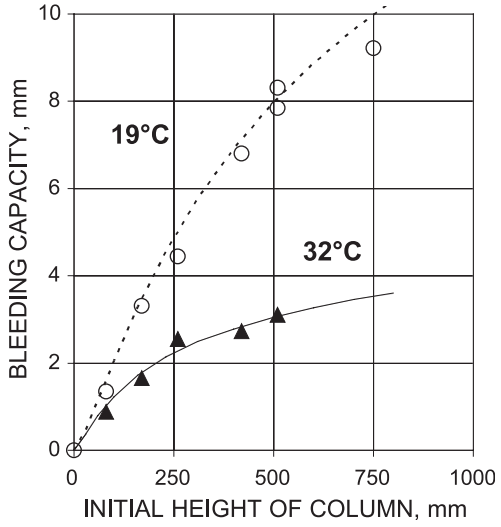

Fig. 7. Influence of the temperature on the ageing effect. Characteristic time of the mortar at 19 °C was 33 min instead of 9 min at 32 °C.

As it is well known, the cement hydration is strongly influenced by temperature so that the ageing effect increases with temperature as reported in Fig. 7 (see also Ref. [5]). The characteristic ageing time also increases with the retarding agent. Indeed, with the retarding agent we used in Ref. [3], the characteristic time was found to be 30 and 18 min in the absence of retarder. Plasticizer and high water reducer lower the strength of the physical interactions and likely result in the increase of the characteristic time. Although there is still only few data available at the time being for comparison, experimental results reported in Table 2 reveal a twofold increase with the high-range water reducer.

Finally, mineral admixture may have also an influence. When totally replacing the cement of a mortar by a coal fly ash and subsequently by a limestone filler [3], the characteristic time was found to be, respectively, 33 min in the case of fly ash and 230 min in the case of limestone filler, compared to 15 min in the case of cement as fine particles. Note that fly ash in water, although possibly not chemically reactive, can increase the physical interactions by releasing Al^{3+} ions in solution.

5. Conclusion

In this paper, we proposed a new bleeding model to account for the ageing effect occurring before the actual setting of concrete. This model is based upon a self-weight consolidation model involving the compressibility of the granular skeleton. This compressibility, as other fresh concrete properties, is an ageing property. Accordingly, a characteristic time has been introduced, which properly scales the ageing kinetics. The assessment of this time

allows us to quantitatively capture various effects. In particular, the amount of cement and the temperature turn out to be the major agents influencing the ageing kinetics.

More research is needed to understand and to capture quantitatively the link between the characteristic time and the mix-design. From a practical point of view, it will then become possible to predict the bleeding, in particular, the one associated with large structures (bridge pylons, piles, etc.) from quick tests performed on small specimens to assess the ageing characteristic time of bleeding.

Notations

C	Maximum solid volume proportion
C_s	Tangent oedometric compressibility
G	Ageing function
H_0	Initial height of the concrete column
K	Current hydraulic conductivity
p	Liquid pressure
t	Time
T_X	Characteristic time scaling the ageing effect
V_s	Velocity of the solid particles
V_{IR}	Rate of bleeding
$V_{IR}(t=0)$	Initial rate of bleeding
z	Current depth of the element
Z	Initial depth of the element
ΔH	Thickness of bleeding water
ΔH_∞	Bleeding capacity
Φ_0	Initial solid volume proportion
Φ	Solid volume proportion in lagrangian coordinate
γ_s	Solid specific weight
γ_w	Water specific weight
φ	Solid volume proportion in eulerian coordinate
λ	Coefficient in the compressibility law
σ	Vertical overall stress
σ'	Terzaghi's effective stress
Ψ_0	Initial fraction of entrapped air

References

[1] T.C. Powers, The Properties of Fresh Concrete, J. Wiley & Sons, New York, USA, 1968, pp. 533–652.

[2] C.K. Loh, T.S. Tan, K.Y. Yong, T.H. Wee, An experimental study on bleeding and channelling of cement paste and mortar, Adv. Cem. Res. 10 (1) (1998 January) 1–16.

[3] L. Josserand, Ressuage des bétons (Bleeding of concrete), PhD thesis of Ecole Nationale des Ponts et Chaussées, 2002, 210 p. (in French).

[4] T.S. Tan, C.K. Loh, K.Y. Yong, T.H. Wee, Modelling of bleeding of cement paste and mortar, Adv. Cem. Res. 9 (34) (1997 April) 75–91.

[5] L. Josserand, F. de Larrard, Experimental study of scale effect in fresh mortar bleeding, Proceedings of the International Congress of Dundee, 2002 (September), pp. 819–826.

[6] E.A. Toorman, Sedimentation and self weight consolidation: general unifying theory, Geotechnique 46 (1) (1996 April) 103–113.

[7] T.S. Tan, T.H. Wee, S.A. Tan, C.T. Tam, S.L. Lee, A consolidation model for bleeding of cement paste, Adv. Cem. Res. 1 (1) (1987) 18–26.

[8] C.A. Clear, D.G. Bonner, Settlement of fresh concrete—an effective stress model, Mag. Concr. Res. 40 (142) (1988 March) 3–12.

[9] L. Josserand, J.P. Ildefonse, F. de Larrard, Perméabilité à l'eau des suspensions granulaires: application au ressuage du béton frais (Water permeability of granular suspensions—application to fresh concrete bleeding), Bull. Lab. Ponts Chaussées 241 (2003) 61–70 (in French).

[10] L. Josserand, F. de Larrard, A method for concrete bleeding measurement, Mat. Struct. 37 (274) (2004 December) 666–670.

[11] F. de Larrard, Concrete mixture-proportioning—a scientific approach, Modern Concrete Technology Series, vol. 9, E&F N SPON, London, 1999, 441 pp.